Semimetal with both Rarita-Schwinger-Weyl and Weyl excitations

Long Liang[1,2] and Yue Yu[1,3]

[1]*Department of Physics, Center for Field Theory and Particle Physics, State Key Laboratory of Surface Physics and Collaborative Innovation Center of Advanced Microstructures, Fudan University, Shanghai 200433, China*

[2]*COMP Centre of Excellence, Department of Applied Physics, School of Science, Aalto University, FI-00076 Aalto, Finland*

[3]*State Key Laboratory of Theoretical Physics, Institute of Theoretical Physics, Chinese Academy of Sciences, P.O. Box 2735, Beijing 100190, China*

(Received 22 June 2015; revised manuscript received 23 December 2015; published 12 January 2016)

A relativistic spinor with spin 3/2 is historically called a Rarita-Schwinger spinor. The right- and left-handed chiral degrees of freedom for the massless Rarita-Schwinger spinor are independent and are thought of as the left and right Weyl fermions with helicity $\pm 3/2$. We study three orbital spin-1/2 Weyl semimetals in the strong spin-orbital coupling limit with time reversal symmetry breaking. We find that in this limit the systems can be a $J_{\text{eff}} = 1/2$ Weyl semimetal or a $J_{\text{eff}} = 3/2$ semimetal, depending on the Fermi level position. The latter near Weyl points includes degrees of freedom of both Rarita-Schwinger-Weyl and Weyl. A nonlocal potential separates the Weyl and Rarita-Schwinger-Weyl degrees of freedom, and a relativistic Rarita-Schwinger-Weyl semimetal emerges. This recipe can be generalized to a mulit-Weyl semimetal and Weyl fermions with pairing interaction to obtain high monopole charges. Similarly, a spatial-inversion-breaking Raita-Schwinger-Weyl semimetal may also emerge.

DOI: 10.1103/PhysRevB.93.045113

I. INTRODUCTION

In 1936, eight years after derived his famous relativistic electron equations of motion, Dirac generalized these equations to higher spin relativistic particles [1]. The first important example was the recovering of Maxwell's equations. The next simplest particle except the electron and the photon is of spin 3/2 and obeys so-called Rarita-Schwinger (RS) equations [2]. This fermonic field later played an important role in supergravity theory, and is known as the superpartner of the graviton, the gravitino [3].

Electrons and photons are particles accompanying us in daily life, while the RS particles are not found even in experiments of high energy physics or in cosmology observations. Recently, the interplay between high energy physics and condensed matter physics supplied a new framework to the relativistic systems: e.g., Dirac semimetals in graphene [4] and three dimensions [5–7], topological insulators [8,9], supersymmetric systems [10–13], and the newly proposed [14] and discovered [15–21] Weyl semimetal. To our knowledge, the RS physics was not relevant in the condensed matter and cold atom context. Can we expect a RS or RS-Weyl semimetal in this new framework?

The RS spinor can consist of the product of a spin-1 vector and a spin-1/2 Dirac spinor. The product can be decomposed into spin-3/2 and spin-1/2 irreducible representations of a Lorentz group. After projecting to the spin-3/2 representation, this is the RS theory. The massless relativistic systems with spin > 0 possess only two physical degrees of freedom: the highest and lowest helicity states [22]. The Maxwell field with only transverse components is a well-known example. There are also only two independent solutions of the massless RS equations: the right- and left-handed chiral modes associated with helicity $\pm 3/2$. This is a result of the Lorentz invariance and gauge invariance of the massless relativistic theory with spin $> 1/2$.

Emergent Weyl fermions in condensed matter systems were first recognized in the fermionic spectrum of superfluid ^{3}He-A and also in the core of quantized vortices in ^{3}He-B [23]. The earlier theoretical prediction of a Weyl semimetal was based on the $J_{\text{eff}} = 1/2$ states in iridates [14] which belong to a large class of $4d$ and $5d$ transition metal oxides with a strong spin-orbital coupling. When the d orbitals are below 2/3 filling, the crystal field projects the electron configurations to the t_{2g} orbitals. When the strong spin-orbital coupling dominates, the electrons fill the $J_{\text{eff}} = 1/2$ or $J_{\text{eff}} = 3/2$ band depending on the filling factor. For iridates, the $5d^5$ electrons occupy all $J_{\text{eff}} = 3/2$ states and half fill the $J_{\text{eff}} = 1/2$ orbitals [24]. For $d^{1,2}$ electrons, they quarter or half occupy the $J_{\text{eff}} = 3/2$ states. The representatives of these $J_{\text{eff}} = 3/2$ materials are the ordered double perovskites with the chemical formula $A_2B'BO_6$, where B' ions are commonly $4d^{1,2}$ and $5d^{1,2}$ transition metals, e.g., Mo^{+5}, Re^{+6}, Os^{+7} for d^1 and Re^{+5}, Os^{+6} for d^2. Several exotic magnetic phases and a quadrupolar phase were presented in these strongly correlated materials [24–26]. Such $J_{\text{eff}} = 3/2$ systems may also exist in p-orbital electrons of antiperovskites materials, A_3BX [27], as well as in cold atom systems [28].

We do not yet know in what kind of materials or cold atom systems the RS physics can exist. In this paper, we present a recipe to realize the RS-Weyl semimetal from three orbital Weyl semimetals with a strong on-site spin-orbital coupling. Each copy of the Weyl semimetal breaks time reversal symmetry (TRS) and possesses helicity, say 1/2 at a right-handed Weyl point. We consider a large spin-orbital coupling limit of our model in order to understand the RS physics included in this system. In this limit, the on-site spin-orbital coupling is taken as an unperturbed Hamiltonian, and the zero-order states are the eigenstates of the total on-site angular momentum $\mathbf{J}$. There is a large energy gap between the $J = 3/2$ and 1/2 states. Projecting the three copies of a Weyl semimetal to $J = 1/2$, we have a single copy of the Weyl semimetal with opposite helicity. Projecting to $J = 3/2$, there are two pairs of linear dispersions with different Fermi velocities. The steeper dispersion is $|\mathbf{P}|$ while

the flat dispersion is $|\mathbf{P}|/3$. Their helicities are $3/2$ and $1/2$ and yield the RS-Weyl and Weyl excitations, respectively. The Berry phases of helicity $3/2$ and $1/2$ states possess topological monopoles with charges $C = 3$ and $C = 1$, respectively, for an original $C = 1$ Weyl point. To split the degeneracy between the RS-Weyl degrees of freedom with helicity $3/2$ and the Weyl degrees of freedom with helicity $1/2$, a nonlocal potential is needed. *A RS-Weyl semimetal emerges in the helicity 3/2 band*. Two generalizations directly follow: we can apply this recipe to double Weyl fermions [29–31] and to ^{3}He-A with a triplet p wave pairing [23,32]. We also study a RS-Weyl semimetal model with space inversion symmetry (SIS) breaking. Projecting to $J_{\text{eff}} = 3/2$, we find the same projected model as that in the TRS breaking systems.

This paper was organized as follows. In Sec. II, we will give a recipe for a RS-Weyl semimetal with TRS breaking. In Sec. III, the generalizations and similarity with SIS breaking mentioned in the preceding paragraph are studied. Section IV contains our conclusions and discussions.

II. RECIPE FOR A $J_{\text{eff}} = 3/2$ SEMIMETAL WITH TRS BREAKING

In this section, we study a RS-Weyl fermion with TRS breaking.

A. Rarita-Schwinger equations

We briefly introduce the RS equations. The RS equations for a sixteen-component vector-spinor field $\psi_{\mu\alpha}$ in 3+1 dimensions are given by

$$(i\gamma^\mu\partial_\mu - m)\psi_\nu = 0, \tag{1}$$

$$\chi = \gamma^\mu\psi_\mu = 0, \tag{2}$$

where the conventions we use are as follows: $\mu = 0,a$ ($a = 1,2,3$) denote the time-space indices with flat metric $\eta^{00} = \eta_{00} = 1$ and $\eta_{aa} = -\eta^{aa} = -1$; $\alpha = s\sigma$ for $s = R,L$ and $\sigma = \uparrow,\downarrow$ are chiral and spin indices, respectively. γ^μ are the gamma matrices. In Eq. (2), the four-vector indices are summed over so that χ is a pure Dirac spinor. $\chi = 0$ projects out the spin-$1/2$ sector and leaves only the degrees of freedom of the spin-$3/2$ sector. It is known that, if $m \neq 0$, there will be fermonic modes with superluminal velocities if the RS field couples to the external electromagnetic field in a minimal way [33,34]. A massless RS theory is gauge invariant under $\psi_\mu \to \psi_\mu + \partial_\mu\epsilon$ for an arbitrary spinor ϵ. The gauge invariance of massless RS theory allowed us to take the $\psi_0 = 0$ gauge, like taking the $A_0 = 0$ gauge for the electromagnetic field. Also similar to Maxwell's theory, only the transverse fields are physical degrees of freedom, namely, $\partial_i\psi^i = 0$. These transverse spinor fields are the right-handed (left-handed) fields with helicity $3/2$ ($-3/2$) [22,35]. We call them the right-handed (left-handed) RS-Weyl fields $c_{aR(L)\sigma}$ if we write the four-component spinor $\psi_a^\dagger = (c_{aL\sigma}^\dagger, c_{aR\sigma}^\dagger)$. Fourier modes of ψ_a are denoted as $(c_{\pm3/2,p}\mathcal{U}_{aR(L)\sigma}, d_{\pm3/2,p}^\dagger\mathcal{V}_{aR(L)})$ where $c_{\pm3/2,p}$ and $d_{\pm3/2,p}^\dagger$ are the particle and antiparticle modes with helicity $\pm3/2$. $\mathcal{U}_{R(L)a}$ and $\mathcal{V}_{R(L)a}$ are two-component spinors for a given a; they are normalized by $\mathcal{U}_L^{a\dagger}\sigma^b\mathcal{U}_{aR} = \mathcal{V}_L^{a\dagger}\sigma^b\mathcal{V}_{aR} = -p^b/p_0$ and $\mathcal{U}_{R(L)}^{a\dagger}\mathcal{V}_{aR(L)} = 0$. Notice that $\mathcal{U}$ and $\mathcal{V}$ are not independent but are related by the charge conjugation. The dispersions of these traverse modes are linear, i.e., $E = p_0 = |\mathbf{p}|$, as expected [22].

B. Recipe for $J_{\text{eff}} = 3/2$ semimetal with TRS breaking

We now dispense a recipe for the RS-Weyl semimetal from a three orbital Weyl semimetal, with help of a strong on-site spin-orbital coupling. The Hamiltonian describes three copies of a Weyl semimetal on a three-dimensional lattice, i.e.,

$$H = \sum_{abc\sigma\sigma'\mathbf{p}} c_{a\mathbf{p}\sigma}^\dagger\left[P_c(\mathbf{p})\delta_{ab}\sigma_{c\sigma\sigma'} - \lambda L_{ab}^c\sigma_{c\sigma\sigma'}\right]c_{b\sigma'\mathbf{p}}, \tag{3}$$

where the on-site orbital angular momentum matrix is defined by $L^1 = T^1$, $L^2 = -T^2$, and $L^3 = -T^3$ with $T_{ab}^c = -i\epsilon_{abc}$; the second term in (3) is the on-site spin orbital coupling. We here assume $\lambda > 0$. For any given a, $\mathbf{P}(\mathbf{p})\cdot\boldsymbol{\sigma}$ in (3) describes a spin-$1/2$ Weyl semimetal with the TRS breaking in a condensed matter or cold atom system [14]. Namely, near any right- or left-handed chiral Weyl point $\mathbf{p}_w$, $\mathbf{P}\cdot\boldsymbol{\sigma} \approx \pm v_F(\mathbf{p} - \mathbf{p}_w)\cdot\boldsymbol{\sigma}$. For example, $P^1 = t\sin p_1$, $P^2 = t\sin p_2$, $P^3 = 2t(\cos p_3 - \cos p_0) + m(2 - \cos p_1 - \cos p_2)$, which describe the Weyl semimetal in iridates $A_2\text{Ir}_2\text{O}_7$ [36]. Equation (3) is a single-particle Hamiltonian and can be diagonalized. The dispersions of six branches are given by

$$E = \pm|\mathbf{P}| - \lambda, \tag{4}$$

$$E = \tfrac{1}{2}[\pm\sqrt{9\lambda^2 + 4(\mathbf{P}^2 \pm \lambda|\mathbf{P}|)} + \lambda]. \tag{5}$$

The spin-orbital coupling lifts the degeneracy of the three identical Weyl semimetals while the Weyl points are the same as those in a single copy of the Weyl semimetal. For a vanishing spin-orbital coupling, i.e., $\lambda < 1/L$ where L is the system size, (5) reduces to $\pm|\mathbf{P}| + O(1/L)$. Each copy of the semimetal contributes a monopole charge $C = 1$ of the Berry phase of the wave function surrounding a right-handed chirality Weyl point. However, the vanishing spin-orbital coupling is an isolated point. For any finite λ, i.e., $\lambda > 1/L$, the energy of two branches of (5) near the Weyl points rises by 2λ, while the energy of the other two branches lowers by $-\lambda$, the same as that in (4). We calculate the monopole charges by using P^a in [36]. For a right-handed Weyl point $(0,0,p_0)$, instead of $C = 1$ when $p_z \in (-p_0, p_0)$, the charge corresponding to (4) becomes $C = 3$. A $C = \pm1$ monopole-antimonopole pair develops, corresponding to (5). The antimonopole has a higher energy, 2λ, while the monopole with $C = 1$ has the same energy as that with $C = 3$. If λ is larger enough, say, the order of the bandwidth, the $C = 1,3$ branches and $C = -1$ branches are separated into two bands: a lower band and a upper band, respectively.

The monopole charges of a Weyl point for a finite λ can be determined in the large-λ limit, which is not model dependent. One can also see the RS degrees of freedom in this limit. We take the spin-orbital coupling term as the unperturbed Hamiltonian, denoted as H_0, and the Weyl semimetal part in (3) as the perturbed Hamiltonian H_1. The total on-site angular momentum matrix $\mathbf{J}_{a\sigma,b\sigma'} = \mathbf{L}_{ab}\delta_{\sigma\sigma'} + \frac{1}{2}\delta_{ab}\boldsymbol{\sigma}_{\sigma\sigma'}$ commutes with the unperturbed Hamiltonian matrix $\mathcal{H}_0 = -\lambda L_{ab}^c\sigma_{c\sigma\sigma'}$. The unperturbed wave functions are then the eigenstates of $|\mathbf{J}|$.

The eigenvalues of $|\mathbf{J}|$ are $J = 1/2$ and $3/2$ and the basis of unperturbed state spaces is given by

$$\begin{bmatrix} \left|\frac{1}{2},\frac{1}{2}\right\rangle \\ \left|\frac{1}{2},\frac{-1}{2}\right\rangle \\ \left|\frac{3}{2},\frac{3}{2}\right\rangle \\ \left|\frac{3}{2},-\frac{3}{2}\right\rangle \\ \left|\frac{3}{2},\frac{1}{2}\right\rangle \\ \left|\frac{3}{2},-\frac{1}{2}\right\rangle \end{bmatrix} = \begin{bmatrix} 0 & \frac{1}{\sqrt{3}} & 0 & \frac{i}{\sqrt{3}} & \frac{1}{\sqrt{3}} & 0 \\ \frac{1}{\sqrt{3}} & 0 & \frac{-i}{\sqrt{3}} & 0 & 0 & \frac{1}{\sqrt{3}} \\ \frac{-1}{\sqrt{2}} & 0 & \frac{-i}{\sqrt{2}} & 0 & 0 & 0 \\ 0 & \frac{1}{\sqrt{2}} & 0 & \frac{-i}{\sqrt{2}} & 0 & 0 \\ 0 & \frac{-1}{\sqrt{6}} & 0 & \frac{-i}{\sqrt{6}} & \sqrt{\frac{2}{3}} & 0 \\ \frac{1}{\sqrt{6}} & 0 & \frac{-i}{\sqrt{6}} & 0 & 0 & \sqrt{\frac{2}{3}} \end{bmatrix} \begin{bmatrix} |1,\uparrow\rangle \\ |1,\downarrow\rangle \\ |2,\uparrow\rangle \\ |2,\downarrow\rangle \\ |3,\uparrow\rangle \\ |3,\downarrow\rangle \end{bmatrix}. \tag{6}$$

The unperturbed energies are 2λ and $-\lambda$, corresponding to $J = 1/2$ and $J = 3/2$, respectively. In the large-λ limit, there is a large energy gap $\sim 3\lambda$ between the $J = 1/2$ upper band and the $J = 3/2$ lower band. The projected matrices of any 6×6 matrix $\mathcal{O}$ are defined by

$$\mathcal{O}_{1/2} = \mathcal{P}_{1/2}^{\dagger}\mathcal{O}\mathcal{P}_{1/2}, \quad \mathcal{O}_{3/2} = \mathcal{P}_{3/2}^{\dagger}\mathcal{O}\mathcal{P}_{3/2}, \tag{7}$$

where the project matrices are given by

$$\mathcal{P}_{1/2} = \begin{bmatrix} 0 & \frac{1}{\sqrt{3}} \\ \frac{1}{\sqrt{3}} & 0 \\ 0 & \frac{i}{\sqrt{3}} \\ \frac{-i}{\sqrt{3}} & 0 \\ \frac{1}{\sqrt{3}} & 0 \\ 0 & \frac{1}{\sqrt{3}} \end{bmatrix}, \quad \mathcal{P}_{3/2} = \begin{bmatrix} \frac{-1}{\sqrt{2}} & 0 & 0 & \frac{1}{\sqrt{6}} \\ 0 & \frac{1}{\sqrt{2}} & \frac{-1}{\sqrt{6}} & 0 \\ \frac{i}{\sqrt{2}} & 0 & 0 & \frac{i}{\sqrt{6}} \\ 0 & \frac{i}{\sqrt{2}} & \frac{i}{\sqrt{6}} & 0 \\ 0 & 0 & \sqrt{\frac{2}{3}} & 0 \\ 0 & 0 & 0 & \sqrt{\frac{2}{3}} \end{bmatrix}. \tag{8}$$

Projecting to $J_{\text{eff}} = 1/2$, we have an effective Weyl semimetal described by the Hamiltonian

$$\mathcal{H}_{1/2} = \frac{1}{3}\begin{bmatrix} -P_3 & P_- \\ P_+ & P_3 \end{bmatrix}. \tag{9}$$

It is a single copy of the Weyl semimetal with opposite helicity to the original Weyl semimetal. If we neglect the second-order correction $O(|\mathbf{P}|^2/\lambda)$, the spectrum of the $J_{\text{eff}} = 1/2$ system is simply

$$E_{1/2,\pm 1/2} = \pm|\mathbf{P}|/3 + 2\lambda.$$

Projecting to $J_{\text{eff}} = 3/2$, one finds that $\mathbf{L}_{3/2} = \mathcal{P}_{3/2}^{\dagger}(\mathbf{L}_{ab}\delta_{\sigma\sigma'})\mathcal{P}_{3/2}$ obeys the commutation relation

$$\left[\frac{3}{2}L_{3/2}^{a}, \frac{3}{2}L_{3/2}^{b}\right] = \sum_{c=1}^{3} i\epsilon^{abc}\frac{3}{2}L_{3/2}^{c}.$$

That is, $J_{\text{eff}}^{a} = \frac{3}{2}L_{3/2}^{a}$ are the SU(2) $J_{\text{eff}} = 3/2$ generators. In fact, the projected orbital and spin matrices are equal,

$$\mathcal{P}_{3/2}^{\dagger}(\mathbf{L}_{ab}\delta_{\sigma\sigma'})\mathcal{P}_{3/2} = \mathcal{P}_{3/2}^{\dagger}(\delta_{ab}\boldsymbol{\sigma}_{\sigma\sigma'})\mathcal{P}_{3/2}. \tag{10}$$

Namely, the projected effective total on-site angular momentum matrix is given by

$$\begin{aligned}\mathbf{J}_{3/2} &= \mathcal{P}_{3/2}^{\dagger}(\mathbf{L}_{ab}\delta_{\sigma\sigma'})\mathcal{P}_{3/2} + \tfrac{1}{2}\mathcal{P}_{3/2}^{\dagger}(\delta_{ab}\boldsymbol{\sigma}_{\sigma\sigma'})\mathcal{P}_{3/2} \\ &= \tfrac{3}{2}\mathcal{P}_{3/2}^{\dagger}(\mathbf{L}_{ab}\delta_{\sigma\sigma'})\mathcal{P}_{3/2} = \tfrac{3}{2}\mathbf{L}_{3/2}.\end{aligned} \tag{11}$$

This exactly gives rise to $\mathbf{J}_{3/2} = \mathbf{J}_{\text{eff}}$, and the projected Hamiltonian $\mathcal{H}_{3/2} = \mathcal{P}_{3/2}^{\dagger}\mathcal{H}_1\mathcal{P}_{3/2}$ reads

$$\mathcal{H}_{3/2} = \mathbf{P}\cdot\mathbf{L}_{3/2} = \frac{2}{3}\mathbf{P}\cdot\mathbf{J}_{3/2} = \begin{bmatrix} P_3 & 0 & \frac{P_-}{\sqrt{3}} & 0 \\ 0 & -P_3 & 0 & \frac{P_+}{\sqrt{3}} \\ \frac{P_+}{\sqrt{3}} & 0 & \frac{P_3}{3} & \frac{2P_-}{3} \\ 0 & \frac{P_-}{\sqrt{3}} & \frac{2P_+}{3} & -\frac{P_3}{3} \end{bmatrix} \tag{12}$$

where $P_{\pm} = P_1 \pm iP_2$.

Neglecting the higher order correction, the dispersions of $\mathcal{H}_{3/2} + \mathcal{H}_0$ are given by

$$E_{3/2,\pm 3/2} = \pm|\mathbf{P}| - \lambda, \tag{13}$$

$$E_{3/2,\pm 1/2} = \pm|\mathbf{P}|/3 - \lambda. \tag{14}$$

We see that the Weyl points are not shifted.

C. Helicity and RS-Weyl semimetal

The large-λ perturbed dispersions $E_{1/2,\pm 1/2}$, $E_{3/2,\pm 3/2}$, and $E_{3/2,\pm 1/2}$ are of course consistent with the exact results (4) and (5). However, the simple Hamiltonians in the large λ limit may explicitly give rise to more information. The gapless linear dispersions imply that theeigen states are not the eigenstates of $\mathbf{J}_{\text{eff}}$: they are the eigenstates of the helicity operator. For $J_{\text{eff}} = 1/2$, the helicity operator is the same as that of the usual Weyl semimetal. Here we consider the case of $J_{\text{eff}} = 3/2$. We define an operator $\mathfrak{h} = \hat{\mathbf{P}}\cdot\mathbf{J}$ with $\hat{\mathbf{P}} = \frac{\mathbf{P}}{|\mathbf{P}|}$. Projecting to $J_{\text{eff}} = 3/2$, the projected helicity operator is $\mathfrak{h}_{3/2} = \mathcal{P}_{3/2}\hat{\mathbf{P}}\cdot\mathbf{J}\mathcal{P}_{3/2} = \hat{\mathbf{P}}\cdot\mathbf{J}_{3/2}$, i.e., the projected helicity operator matrix is given by

$$h_{3/2} = \frac{3}{2|\mathbf{P}|}\mathcal{H}_{3/2}. \tag{15}$$

This means that the projected helicity operator commutes with the Hamiltonian $H_{3/2}$. The states with dispersion $E = \pm|\mathbf{P}|$ are the helicity eigenstates with $h_{3/2} = \pm 3/2$, while the states with $E = \pm|\mathbf{P}|/3$ have helicity $\pm 1/2$. The corresponding monopole charges then are $C = 3$ and $C = 1$ for the right-handed Weyl point, recovered in our calculation before. The total monopole charge in the $J_{\text{eff}} = 3/2$ band is $C = 4$.

The helicity $\pm 3/2$ states give the RS-Weyl degrees of freedom in the $J_{\text{eff}} = 3/2$ band. Since $C = 4$ is a topologically invariant, any local perturbation cannot split the helicity $1/2$ sector from the $3/2$ sector in the lower band. One can add a nonlocal potential to lift this degeneracy, e.g.,

$$V = U\sum_{\mathbf{p},ij} c_{\mathbf{p}}^{\dagger}h_{3/2}^{2}(\mathbf{p})c_{\mathbf{p}} \propto \sum_{\mathbf{p},ij}\frac{P_a P_b}{|\mathbf{P}|^2}c_{i\mathbf{p}}^{\dagger}\left[J_{3/2}^{a}J_{3/2}^{b}\right]_{ij}c_{j\mathbf{p}},$$

where U is a constant; i and j label four states with $J_{\text{eff}}^{z} = \pm 1/2, \pm 3/2$. This potential lifts the energy $E_{3/2,\pm 3/2} \to E_{3/2,\pm 3/2} + 9U/4$ and $E_{3/2,\pm 1/2} \to E_{3/2,\pm 1/2} + U/4$. Therefore, if $\lambda > |U| >$ bandwidth, the lower band is separated into a $h_{3/2} = \pm 1/2$ sub-band and a $h_{3/2} = \pm 3/2$ sub-band. When the Fermi energy is in the band of helicity $\pm 3/2$, the low-lying excitations near each Weyl point can be thought of as the particles, say $c_{3/2,\mathbf{p}}^{\dagger}$ and antiparticle $d_{3/2,\mathbf{p}}^{\dagger}$; i.e., an

emergent RS-Weyl semimetal. The physical origin of the nonlocal potential (16) needs to be further studied. It may come from a long-range interaction.

In sum, we have offered a recipe for a RS semimetal. The candidates of possible materials are the condensed matter or cold atom systems in which the on-site spin and orbital degrees of freedom are strongly coupled.

III. GENERALIZATIONS TO WEYL FERMIONS WITH SIS BREAKING, THE MULTIDEGENERACY, AND PAIRED WAVE FUNCTION

We now study the generalizations of our recipe to other systems: the Weyl fermions with SIS breaking, the multidegeneracy, and paired wave function.

A. With SIS breaking

The Weyl semimetal breaks either TRS or SIS. We can also start from a SIS breaking Weyl semimetal. We study the Hamiltonian

$$H_1' = \sum_{abc\sigma\mathbf{p}} c^\dagger_{a\sigma\mathbf{p}} L^c_{ab} P_c c_{b\sigma\mathbf{p}}. \tag{16}$$

Instead of Pauli matrices in H_1, which breaks the TRS, $\mathbf{L}$ connects the different orbital degrees of freedom in H_1' and then breaks SIS. The model $H_0 + H_1'$ can also be analytically solved. The spectra read

$$E = \pm|\mathbf{P}| - \lambda, \tag{17}$$

$$E = \tfrac{1}{2}[\lambda + |\mathbf{P}| \pm \sqrt{9\lambda^2 + 2\lambda|\mathbf{P}| + \mathbf{P}^2}], \tag{18}$$

$$E = \tfrac{1}{2}[\lambda - |\mathbf{P}| \pm \sqrt{9\lambda^2 - 2\lambda|\mathbf{P}| + \mathbf{P}^2}]. \tag{19}$$

$\lambda = 0$ is also an isolated point. We are interested in finite λ as well. In the strong coupling limit, one has the dispersions $E = \pm|\mathbf{P}| - \lambda$ with $C = 3$, $E = \pm|\mathbf{P}|/3 - \lambda$ with $C = 1$, and $E = \pm 2|\mathbf{P}|/3 + 2\lambda$ with $C = -1$. The physics in each projected band is the same as the cases with TRS breaking.

While there are already several models with TRS breaking [14,36], we here give a toy model for $H_1' + H_0$ in a cubic lattice. The possible physical systems are cold atom gas with p-orbital coupling to pseudospin or $4d^1$ and $5d^1$ electrons with t_{2g} orbital degrees of freedom. The Hamiltonian we are studying is

$$H = -t \sum_{i\sigma} (\pm c^\dagger_{2i\sigma} c_{3,i\pm\delta_x\sigma} \pm c^\dagger_{1i\sigma} c_{2,i\pm\delta_3\sigma} \pm c^\dagger_{1i} c_{3,i\pm\delta_y\sigma}) + \text{H.c.} + H_0, \tag{20}$$

where $\delta_{x,y,z}$ are the lattice vectors in the positive directions. The hopping term is between the different orbitals in different directions. Furthermore, the hopping in the negative δ_i direction carries a phase π while carrying no phase in the positive direction. After Fourier transformation, we have

$$P_a = t \sin p_a.$$

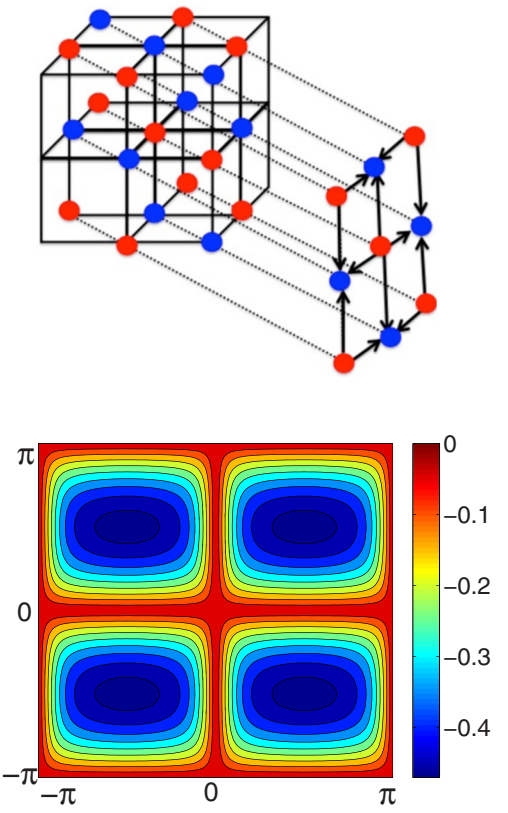

FIG. 1. The dispersions and the Fermi arcs in the [110]-surface Brillouin zone for $t = 1$.Upper: Images of the Weyl points with charges ± 1 (red and blue). Lower: The dispersions and the network of gapless Fermi arcs.

The Weyl points are located in the high symmetric points $\{(0,0,0),(\pi,\pi,\pi)\}$, $\{(0,\pi,\pi),(\pi,0,0)\}$, $\{(\pi,0,\pi),(0,\pi,0)\}$, and $\{(\pi,0,0),(0,0,\pi)\}$. At these Weyl points, the effective Hamiltonian in the long-wavelength limit is exactly the gravitino Hamiltonian in supergravity theory [3].

We study the surface states of this model and consider a surface Brillouin zone with the normal vector along the (n_1,n_2,n_3) direction. The bulk Weyl points are projected onto this surface. A set of the Weyl points may have the same image. The charge of the image is defined by the sum of the winding numbers of these Weyl points in this set divided by the number of the points. It is easy to see the charges of all images are zero if $n_1 + n_2 + n_3$ is odd, while the charges of the images are ± 1 if $n_1 + n_2 + n_3$ is even. For a given surface, these images form a lattice. For a lattice where all sites are zero charged, there is no reason to see the Fermi arc connecting any pair of images, while the Fermi arcs may appear between the positively and negatively charged images in a charged site lattice. In Fig. 1(upper), we sketch the image network for an even surface, the [110] surface. The red and blue spots correspond to the images with charge ± 1. We numerically calculate the surface states of the [001], [111], and [110] surfaces. We see that there is no gapless state for [001] and [111]. The dispersions of the surface states for the [110] are shown in Fig. 1(lower). As expected, the gapless Fermi arcs form a rectangular network and the images are the lattice sites of the network.

B. Multi-Weyl semimetals

We consider a three-dimensional crystal that is invariant under an n-fold rotation about the z axis with $n = 2,3,4,6$. The Hamiltonian is also invariant under C_m if n/m is an integer. If the tight-binding Hamiltonian $H(\mathbf{p}) = \mathbf{P}(\mathbf{p}) \cdot \boldsymbol{\sigma}$ in (3) with translational symmetry [29], C_m invariance gives

$$\hat{C}_m \hat{H}(\mathbf{p}) \hat{C}_m^{-1} = \hat{H}(R_m \mathbf{p}), \tag{21}$$

where $\hat{C}_m$ is the m-fold rotation operator and R_m is the 3×3 rotation matrix. Equation (3) defines three copies of a multi-Weyl semimetal around a Weyl node through a strong spin-orbital coupling. After projecting to $J_{\text{eff}} = 3/2$, we define a multi-RS-Weyl semimetal. For example, we consider a simple tight-binding model with C_4 symmetry given in [31]. In a given Weyl point, the multi-Weyl semimetal Hamiltonian is given by

$$\mathbf{P} \cdot \boldsymbol{\sigma} = \left(p_x^2 - p_y^2\right)\sigma_x + 2p_x p_y \sigma_y + p_z \sigma_z. \tag{22}$$

In this case, the monopole charge is 2 instead of 1. Substituting into Eq. (3), we see that, with the help of strong spin-orbital coupling, three copies of a double Weyl semimetal can also be projected to $J_{\text{eff}} = 1/2$ with monopole charge -2 and $J_{\text{eff}} = 3/2$ with total monopole charge 8. For $J_{\text{eff}} = 3/2$ states, the helicity $3/2$ state has monopole charge 6 and the helicity $1/2$ state has monopole charge 2. If we use the nonlocal potential (16) in Sec. II C, we obtain a multi-RS-Weyl semimetal with monopole charge 6.

C. Weyl fermions with paired wave function in ^{3}He-A

The A-phase of Helium 3 superfluid around a Weyl point can be described by the Bogoliubov—-de Gennes Hamiltonian [32]

$$H = \begin{bmatrix} p_z & 0 & -p_+ & 0 \\ 0 & p_z & 0 & p_+ \\ -p_- & 0 & -p_z & 0 \\ 0 & p_- & 0 & -p_z \end{bmatrix}. \tag{23}$$

There are two degenerate Weyl points with linear dispersion, and the total monopole charge is 2. This is different from the case in the preceding subsection where the dispersion is quadratic in x, y directions. If we couple three copies of this model by strong on-site spin-orbital coupling as before, the projected effective Hamiltonian to $J_{\text{eff}} = 1/2$ states is given by

$$H_{1/2} = \frac{1}{3}\begin{bmatrix} 3p_z & 0 & -p_+ & 0 \\ 0 & 3p_z & 0 & p_+ \\ -p_- & 0 & -3p_z & 0 \\ 0 & p_- & 0 & -3p_z \end{bmatrix}. \tag{24}$$

This has the same monopole charge as Eq. (23), i.e., 2.

Projected to $J_{\text{eff}} = 3/2$ states, the effective Hamilton is given by

$$H_{3/2} = \begin{bmatrix} p_z I_4 & K \\ K^\dagger & -p_z I_4 \end{bmatrix}, \tag{25}$$

where I_4 is a 4×4 unit matrix and

$$K = \begin{bmatrix} 0 & 0 & 0 & p_+/\sqrt{3} \\ 0 & 0 & -p_+/\sqrt{3} & 0 \\ 0 & -p_+/\sqrt{3} & -2p_+/3 & 0 \\ p_+/\sqrt{3} & 0 & 0 & 2p_+/3 \end{bmatrix}. \tag{26}$$

This Hamiltonian is block-diagonal and describes RS fermions with pairing between $(3/2, -1/2)$ and $(-3/2,1/2)$. The eigenenergies are still linear: $\pm|\mathbf{p}|$ and $\pm\frac{1}{3}\sqrt{9p_z^2 + p_x^2 + p_y^2}$, and the monopole charge is 4. Since the paired wave functions are no longer the eigenstates of the helicity, we cannot separate these four dispersions by adding a non local potential (16).

IV. CONCLUSIONS AND DISCUSSIONS

We have given a recipe for realizing the RS-Weyl semimetals from multiple copies of spin-1/2 Weyl fermion matter. $J_{\text{eff}} = 3/2$ chiral fermions are also of two components with helicity $\pm 3/2$. It was easy generalize to the multi-RS-Weyl and paired RS fermions and to obtain higher monopole charge Weyl points.

We did not study the RS or RS-Weyl fermions in 2+1 dimensions. We offer a simple discussion here and leave this to further study. First, the massless RS equations in 2+1 dimensions have a trivial solution. In 2+1 dimensions, the RS spinors ψ_μ ($\mu = 0,1,2$) have two components, and the gamma matrices consist of Pauli matrices: $\gamma^0 = \beta = \sigma^z$, $\gamma^1 = \sigma^z\sigma^x = i\sigma^y$, and $\gamma^2 = \sigma^z\sigma^y = -i\sigma^x$. Solving the supplementary conditions, one has

$$\psi_0 = -\sigma^x\psi_1 - \sigma^y\psi_2, \quad \psi_0 = \frac{i}{E}(\partial_1\psi_1 + \partial_2\psi_2). \tag{27}$$

Due to the gauge invariance, we can take the $\psi_0 = 0$ gauge. Thus, if $\psi_a = \binom{c\chi_a}{\xi_a}$, then

$$\begin{aligned} &\xi_2 = i\xi_1, \quad \chi_2 = -i\chi_1, \\ &\partial_1\chi_1 + \partial_2\chi_2 = 0, \quad \partial_1\xi_1 + \partial_2\xi_2 = 0. \end{aligned} \tag{28}$$

Thus, $\xi_1 = \xi_1(z)$ is holomorphic and $\chi_1 = \chi_1(\bar{z})$ are antiholomorphic because

$$\partial\chi_1 = 0, \quad \bar{\partial}\xi_1 = 0.$$

On the other hand, the Dirac equation for ψ_1 gives

$$E\chi_1(\bar{z}) = \partial\xi_1(z), \quad E\xi_1(z) = \bar{\partial}\chi_1(\bar{z}), \tag{29}$$

and then $\psi_1 = 0$. Finally, we conclude that $\psi_\mu = 0$ and there is only a trivial solution of RS-Weyl equations.

The massive RS equations in 2+1 dimensions, especially their behavior in an external magnetic, field are nontrivial [37]. We will study this in a separate work [38].

ACKNOWLEDGMENTS

The authors thank Gang Chen, Xi Luo, Yong-Shi Wu, and Shiliang Zhu for helpful discussions. This work is supported by the 973 Program of MOST of China (2012CB821402),

the NNSF of China (11174298, 11474061). L.L. is partially supported by the Academy of Finland through its Centres of Excellence Programme (2015-2017) under Project No. 284621.

[1] P. A. M. Dirac, Proc. R. Soc. A **155**, 447 (1936).
[2] W. Rarita and J. Schwinger, Phys. Rev. **60**, 61 (1941).
[3] D. Z. Freedman, P. van Nieuwenhuizen, and S. Ferrara, Phys. Rev. D **13**, 3214 (1976).
[4] A. K. Geim and K. S. Novoselov, Nat. Mater. **6**, 183 (2007).
[5] Z. Liu, B. Zhou, Y. Zhang, Z. Wang, H. Weng, D. Prabhakaran, S.-K. Mo, Z. Shen, Z. Fang, X. Dai, Z. Hussain, and Y. L. Chen, Science **343**, 864 (2014).
[6] M. Neupane, S.-Y. Xu, R. Sankar, N. Alidoust, G. Bian, C. Liu, I. Belopolski, T.-R. Chang, H.-T. Jeng, H. Lin, A. Bansil, F. C. Chou, and M. Z. Hasan, Nat. Commun. **5**, 3786 (2014).
[7] S. Borisenko, Q. Gibson, D. Evtushinsky, V. Zabolotnyy, B. Buchner, and R. J. Cava, Phys. Rev. Lett. **113**, 027603 (2014).
[8] M. Z. Hasan and C. L. Kane, Rev. Mod. Phys. **82**, 3045 (2010).
[9] X.-L. Qi and S.-C. Zhang, Rev. Mod. Phys. **83**, 1057 (2011).
[10] S. S. Lee, Phys. Rev. B **76**, 075103 (2007).
[11] Y. Yu and K. Yang, Phys. Rev. Lett. **105**, 150605 (2010).
[12] T. Grover, D. N. Sheng, and A. Vishwanath, Science **344**, 280 (2014).
[13] S.-K. Jian, Y.-F. Jiang, and H. Yao, Phys. Rev. Lett. **114**, 237001 (2015).
[14] X. Wan, A. M. Turner, A. Vishwanath, and S. Y. Savrasov, Phys. Rev. B **83**, 205101 (2011).
[15] H. Weng, C. Fang, Z. Fang, B. A. Bernevig, and X. Dai, Phys. Rev. X **5**, 011029 (2015).
[16] L. Lu, Z. Wang, D. Ye, L. Ran, L. Fu, J. D. Joannopoulos, and M. Soljacic, Science **349**, 622 (2015).
[17] S.-Y. Xu, I. Belopolski, N. Alidoust, M. Neupane, C. Zhang, R. Sankar, S.-M. Huang, C.-C. Lee, G. Chang, B. Wang, G. Bian, H. Zheng, D. S. Sanchez, F. C. Chou, H. Lin, S. Jia, and M. Z. Hasan, Science **347**, 294 (2015).
[18] B. Q. Lv, H. M. Weng, B. B. Fu, X. P. Wang, H. Miao, J. Ma, P. Richard, X. C. Huang, L. X. Zhao, G. F. Chen, Z. Fang, X. Dai, T. Qian, and H. Ding, Phys. Rev. X **5**, 031013 (2015).
[19] X. Huang, L. Zhao, Y. Long, P. Wang, D. Chen, Z. Yang, H. Liang, M. Xue, H. Weng, Z. Fang, X. Dai, and G. F. Chen, Phys. Rev. X **5**, 031023 (2015).
[20] N. J. Ghimire, Y. Luo, M. Neupane, D. J. Williams, E. D. Bauer, and F. Ronning, J. Phys.: Condens. Matter **27**, 152201 (2015).
[21] C. Shekhar, A. K. Nayak, Y. Sun, M. Schmidt, M. Nicklas, I. Leermakers, U. Zeitler, Z-. K. Liu, Y. L. Chen, W. Schnelle, J. Grin, C. Felser, and B. H. Yan, Nat. Phys. **11**, 645 (2015).
[22] See, e.g., D. Lurie, *Particles and Fields* (John Wiley and Sons, New York, 1968).
[23] G. E. Volovik and V. P. Mineev, JETP **56**, 579 (1982).
[24] For a recent review, see W. Witczak-Krempa, G. Chen, Y. B. Kim, and L. Balents, Annu. Rev. Condens. Matter Phys. **5**, 57 (2014).
[25] G. Chen, R. Pereira, and L. Balents, Phys. Rev. B **82**, 174440 (2010).
[26] G. Chen and L. Balents, Phys. Rev. B **84**, 094420 (2011).
[27] Y. Sun, X-Q. Chen, S. Yunoki, D. Li, and Y. Li, Phys. Rev. Lett. **105**, 216406 (2010); T. Kariyado and M. Ogata, J. Phys. Soc. Jpn. **81**, 064701 (2012); T. H. Hsieh, J. Liu, and L. Fu, Phys. Rev. B **90**, 081112(R) (2014).
[28] Z. Y. Zhou, E. H. Zhao, W. V. Liu, Phys. Rev. Lett. **114**, 100406 (2015).
[29] C. Fang, M. J. Gilbert, X. Dai, B. A. Bernevig, Phys. Rev. Lett. **108**, 266802 (2012).
[30] S.-M. Huang *et al.*, arXiv:1503.05868.
[31] S. K. Jian and H. Yao, Phys. Rev. B **92**, 045121 (2015).
[32] G. E. Volovik, JETP Lett., arXiv:1511.04969.
[33] K. Johnson and E. C. G. Sudarshan, Ann. Phys. **13**, 126 (1961).
[34] G. Velo and D. Zwanziger, Phys. Rev. **186**, 1337 (1969).
[35] A. Das and D. Z. Freedman, Nucl. Phys. B **114**, 271 (1976).
[36] K. Y. Yang, Y. M. Lu, and Y. Ran, Phys. Rev. B **84**, 075129 (2011).
[37] M. Hortasu, Phys. Rev. D **9**, 928 (1974).
[38] X. Luo and Y. Yu (unpublished).